Exploring atom-pairwise and many-body dispersion corrections for the BEEF-vdW functional

View Online   Export Citation   CrossMark

Elisabeth Keller,[1,2] (iD) Volker Blum,[3,4] (iD) Karsten Reuter,[2] (iD) and Johannes T. Margraf[1,2,a] (iD)

AFFILIATIONS

[1] Bavarian Center for Battery Technology (BayBatt) and Chair of Physical Chemistry V, University of Bayreuth, Bayreuth, Germany
[2] Fritz Haber Institute of the Max Planck Society, Berlin, Germany
[3] Thomas Lord Department of Mechanical Engineering and Materials Science, Duke University, Durham, North Carolina 27708, USA
[4] Department of Chemistry, Duke University, Durham, North Carolina 27708, USA

[a] Author to whom correspondence should be addressed: johannes.margraf@uni-bayreuth.de

ABSTRACT

The Bayesian error estimation functional (BEEF-vdW) is widely used in surface science and catalysis, because it provides a balanced description of molecular, surface, and solid state systems, along with reliable error estimates. However, the nonlocal van-der-Waals density functional (vdW-DF2) employed in BEEF-vdW can be computationally costly and displays relatively low accuracy for molecular systems. Therefore, this work explores whether atom-pairwise and many-body dispersion treatments represent viable alternatives to using the vdW-DF2 functional with BEEF-vdW. To this end, we investigate the performance of commonly used atom-pairwise corrections [i.e., the Tkatchenko–Scheffler (TS) and the exchange-hole dipole moment (XDM) approaches] and many-body dispersion (MBD) treatments for molecular, surface, and solid-state systems. The results indicate that atom-pairwise methods such as TS and particularly XDM provide a good balance of cost and accuracy across all systems.

I. INTRODUCTION

Semilocal exchange–correlation (xc) functionals are popular in condensed matter physics and surface science due to their favorable cost–accuracy ratio. However, the simulations of surfaces, interfaces, and catalytic reactions require a balanced description of molecular, surface, and solid state systems, including long-range van der Waals (vdW) interactions. Unfortunately, because of the inherently local nature of semilocal xc functionals, they are not capable of describing long-range correlation effects comprehensively. As a result, additional dispersion treatments must be used to accurately represent dispersion-bound systems. To this end, the total energy of the semilocal DFT method is corrected by a long-range dispersion contribution E_{vdW}. This contribution is most commonly obtained from atom-pairwise corrections,[1–4] many-body dispersion methods,[5,6] or non-local functionals.[7–11] Unfortunately, the interoperability of a given semilocal xc functional and a given long-range dispersion method is not automatically guaranteed but has to be carefully calibrated for molecular, surface, and solid state properties.

A popular general-purpose functional in condensed matter physics and surface science is the BEEF-vdW method proposed by Wellendorff et al.,[12] which consists of a customized semilocal xc functional and the nonlocal vdW-DF2[10] correction. In addition to providing a balanced description of bulk and surface properties, the BEEF-vdW functional provides error estimates, which can be propagated through complex multiscale models.[13] This has, for example, been used for modeling the conversion of exhaust gas emissions from stoichiometric gasoline combustion,[14] catalytic ammonia synthesis,[15] and syngas conversion.[16]

A practical disadvantage of BEEF-vdW is that the evaluation of the nonlocal correlation energy for the vdW-DF2 functional, in principle, requires solving a double integral over the spatial coordinates, unlike the single integral evaluation for the semilocal BEEF functional.[17] This causes additional computational overhead.

While efficient Fast Fourier Transform (FFT) implementations[18] for performing the double integration can reduce this computational cost significantly, they are not available in all electronic structure codes, limiting the availability of the BEEF-vdW method. More fundamentally, however, vdW-DF2 has shown the tendency to overestimate lattice constants and molecule–molecule interactions, creating a case for exploring alternatives to vdW-DF2.[17]

Alternatives to using nonlocal vdW functionals are computationally efficient atom-pairwise dispersion treatments, such as Grimme's D3,[1] D4[19] methods, the Tkatchenko–Scheffler (TS) approach,[2] and the exchange-hole dipole moment (XDM) method.[3,4] There are also various many-body dispersion approaches (MBD@rsSCS and MBD-NL)[5,6,20] that extend this concept beyond pairwise interactions. In this work, we explore whether the performance of the nonlocal vdW-DF2 functional in BEEF-vdW can be emulated or even surpassed by pairwise or many-body dispersion treatments. With this goal in mind, we parameterize the atom-pairwise and many-body dispersion corrections TS, XDM, MBD@rsSCS, and MBD-NL for use with the semilocal part of BEEF-vdW. Subsequently, we explore the performance of the resulting methods for a range of solid state, surface, and adsorbate-surface systems. For the self-consistency of the current paper, the different approaches used are briefly reviewed.

II. THEORY

In the following, the original nonlocal BEEF-vdW functional as described in Ref. [12] will be denoted as BEEF-vdW(DF2). Note that prior to the development of BEEF-vdW(DF2), Mortensen *et al.* reported a related non-dispersion-corrected GGA functional, which is sometimes also termed BEEF.[21] This is distinct from the semilocal xc contribution to the BEEF-vdW functional. For simplicity (and because the original functional by Mortensen *et al.* is not in common use), we will henceforth use the BEEF acronym to refer to the semilocal part of the BEEF-vdW functional. The xc energy of the dispersion corrected BEEF-vdW functional $E_{xc}^{BEEF-vdW(disp)}$ is given by the evaluation of a semilocal xc contribution E_{xc}^{BEEF} and a vdW correction term E_{vdW},[12]

$$E_{xc}^{BEEF-vdW(disp)} = E_{xc}^{BEEF} + E_{vdW}. \tag{1}$$

Evaluations of these BEEF-vdW variants without and with alternative dispersion treatments will be denoted as BEEF-vdW(none), BEEF-vdW(TS), BEEF-vdW(XDM), BEEF-vdW(MBD), BEEF-vdW(MBD-NL), and BEEF-vdW(DF2).
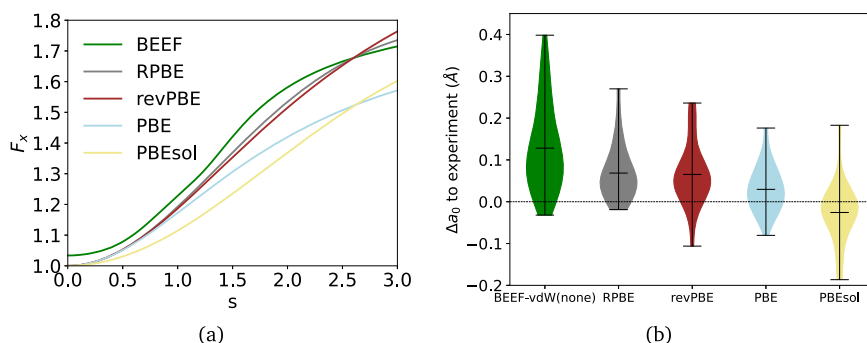
The semilocal contribution is given by

$$E_{xc}^{BEEF} = E_x^{BEEF} + a_c E_c^{LDA} + (1 - a_c)E_c^{PBE}. \tag{2}$$

Here, E_x^{BEEF} is a parameterized GGA exchange functional and a_c is an empirical parameter mixing local and semilocal correlation contributions E_c^{LDA} and E_c^{PBE}.[22,23] As usual, the exchange term E_x^{BEEF} is given by

$$E_x^{BEEF} = \int \epsilon_x^{LDA}(n(\mathbf{r}))F_x^{BEEF}(s)d\mathbf{r}, \tag{3}$$

with the exchange enhancement factor $F_x^{BEEF}(s)$, the electron density $n(\mathbf{r})$, and its reduced density gradient s, which provides a measure of the inhomogeneity of the density by relating the gradient of the electron density $\nabla n(\mathbf{r})$ to $n(\mathbf{r})$,

$$s = \frac{|\nabla n(\mathbf{r})|}{2k_F n(\mathbf{r})} \tag{4}$$

with $k_F = \left(3\pi^2 n(\mathbf{r})\right)^{1/3}$.

The exchange enhancement factor $F_x^{BEEF}(s)$ is given by[12]

$$F_x^{BEEF}(s) = \sum_m a_m B_m\left[\frac{2s^2}{4+s^2} - 1\right], \tag{5}$$

with B_m being the mth-order Legendre polynomials. The exchange coefficients a_m (of which there are $M_x = 30$) are empirically fitted and determine the shape of F_x. This is shown in Fig. 1, compared to other common GGA functionals. Reduced density gradients s within the range of $0 < s \leq 3$ particularly strongly influence the exchange repulsion between non-bonded fragments,[27,28] which must be properly matched to the dispersion correction in order to obtain an accurate description of vdW interactions. For $0 < s \leq 2.5$, $F_x^{BEEF}(s)$ is steeply increasing, leading to a rather repulsive exchange energy contribution similar to other surface-science and molecular functionals, such as revPBE and RPBE; see Fig. 1. The repulsiveness of BEEF exchange has the advantage that nonphysical bonding effects are minimized, which avoids overcorrection and double counting of dispersion contributions. In addition, GGA functionals with steeply rising enhancement factors are known to obtain accurate atomization energies.[29] Meanwhile, combining a functional with a steeply rising exchange enhancement factor, such as revPBE, with nonlocal functionals of the vdW-DF family has

FIG. 1. (a) The exchange enhancement factor F_x as a function of the reduced density gradient s for the BEEF,[12] RPBE,[24] revPBE,[25] PBE,[23] and PBEsol[26] GGA functionals. (b) Performance of BEEF-vdW(none) compared to RPBE, revPBE, PBE, and PBEsol for lattice constants of 25 covalently bound and metallic crystals from Sol27Lc.[12]

shown to cause systematic overestimation of intermolecular binding distances, molecule-to-surface adsorption distances, and lattice constants.[30–33] Conversely, less repulsive functionals such as PBE and PBEsol tend to overestimate lattice constants less or may even underestimate them.[34]

A. Nonlocal vdW-DF2 dispersion treatment

BEEF-vdW(DF2) uses vdW-DF2[10] to compute the dispersion contribution E_{vdW}. This functional is part of a family of nonlocal functionals[9,10,35] based on the local polarizability approximation, originally developed for layered systems.[8,36,37] In principle, it can be seamlessly combined with any semilocal functional. However, the performance of the combined method strongly depends on the properties of the underlying functional.[38]

The functionals of the vdW-DF family use the dielectric response of the uniform electron gas (UEG) with electron density $n(r)$ to compute a nonlocal correlation contribution derived from the adiabatic connection formula (ACF),[8,9,37]

$$E_c^{nl} = \int_0^\infty \frac{1}{2\pi} \, \text{tr}[\ln(1 - V\tilde{\chi}) - \ln \epsilon(\omega)] \frac{d(-i\omega)}{2\pi}, \quad (6)$$

with $i\omega$ denoting the imaginary frequencies, $\tilde{\chi}$ being the density response to a self-consistent potential with interfragment contributions removed,[37] V being the electron–electron Coulomb interaction, and $\epsilon(\omega)$ being the dielectric function. Equation (6) can be expanded to second order in terms of the effective plasmon propagator S_{xc} with $\epsilon(\omega) = e^{S_{xc}(\omega)} \approx 1 + S_{xc}(\omega) + \frac{S_{xc}(\omega)^2}{2!}$ and using the Fourier transform of S_{xc}, to obtain[9,35]

$$E_c^{nl}[n] \approx \iiint \left[1 - (\hat{\mathbf{q}} \cdot \hat{\mathbf{q}}')^2\right] S_{xc}(\mathbf{q}, \mathbf{q}'; \omega)$$
$$\times S_{xc}(\mathbf{q}', \mathbf{q}; \omega) d^3\mathbf{q}' d^3\mathbf{q} \frac{d(-i\omega)}{4\pi}. \quad (7)$$

This equation can be rewritten using a kernel $\phi[n](\mathbf{r}, \mathbf{r}')$, describing the effective interaction between the electron density at two points in space $n(\mathbf{r}')$ and $n(\mathbf{r}')$,[7,9,10]

$$E_c^{nl}[n] = \frac{1}{2} \iint n(\mathbf{r})\phi[n](\mathbf{r}, \mathbf{r}')n(\mathbf{r}') d^3\mathbf{r}' d^3\mathbf{r}. \quad (8)$$

To develop computationally tractable expressions of the interaction kernel ϕ, vdW functionals approximate the effective plasmon propagator, typically using appropriate expressions for the plasmon frequency $\omega_\mathbf{q}(\mathbf{r})$. Different approximations for $\omega_\mathbf{q}(\mathbf{r})$ exist, leading to various nonlocal vdW functionals, including vdW-DF1, vdW-DF2, vdW-DF3, as well as VV09[39] and VV10.[40] For vdW-DF2, the plasmon dispersion is rewritten in terms of $\mathbf{q}_0(\mathbf{r})$, which is given by[9,10,35]

$$\mathbf{q}_0(\mathbf{r}) = \frac{\epsilon_{xc}^{int}(\mathbf{r})}{\epsilon_x^{LDA}} k_F(\mathbf{r}). \quad (9)$$

Here, the internal GGA functional $\epsilon_{xc}^{int}(\mathbf{r})$ is approximated by an LDA exchange–correlation contribution and a quadratic gradient correction,[9,10,35]

$$\epsilon_{xc}^{int}(\mathbf{r}) = \epsilon_{xc}^{LDA} - \epsilon_{xc}^{LDA} Z_{ab} \frac{s^2}{9}. \quad (10)$$

vdW-DF1 and vdW-DF2 only differ by the gradient coefficient Z_{ab}.[9,10] For vdW-DF1, $Z_{ab} = -0.8491$ is used, which was parameterized for use with the revPBE functional.[9,41] vdW-DF1 gives reliable results for adsorbed molecules and solid-state materials but overestimates molecule–molecule interaction distances.[17] This deficiency for molecule–molecule interactions is somewhat reduced by using vdW-DF2, which simply entails setting $Z_{ab} = -1.887$ in the internal functional designed for the less repulsive PW86R[28,42] exchange functional.[10,35] However, this reparameterization causes vdW-DF2 to underestimate dispersion coefficients more than other vdW-DF methods.[36]

B. Atom-pairwise and many-body dispersion methods

A variety of atom-pairwise and many-body dispersion methods are known in the literature. Herein, we focus on the TS[2] and XDM[3,4] methods as representative atom-pairwise treatments, as well as the MBD@rsSCS[5] and MBD-NL[6] many-body methods.

1. Dispersion energy of interacting quantum harmonic oscillators

Atom-pairwise and many-body dispersion treatments are based on the long-range description of the dipole–dipole dispersion energy from interacting quantum harmonic oscillators (QHOs) of charge densities, which are used to model polarizable atoms in a molecule or a material.[43,44] The dipole–dipole dispersion energy $E_{disp,ab}$ between two atoms a, b can be described by the instantaneous interaction between two QHOs with imaginary angular frequency $i\omega$,[45]

$$E_{disp,ab} = -\frac{\hbar}{2\pi} \sum_{\alpha\gamma\beta\delta} T_{ab}^{\alpha\gamma} T_{ab}^{\beta\delta} \int_0^\infty \alpha_a^{\alpha\beta}(i\omega)\alpha_b^{\gamma\delta}(i\omega) d\omega. \quad (11)$$

Here, $\alpha_a^{\alpha\beta}$ and $\alpha_b^{\gamma\delta}$ represent the polarizability tensors of atoms a and b, respectively. $T_{ab}^{\alpha\gamma}$ and $T_{ab}^{\beta\delta}$ are interaction tensors describing the dipole interaction between sites $\mathbf{R}_a$ and $\mathbf{R}_b$ given by[45]

$$T_{ab}^{\alpha\beta} = \nabla_\alpha \nabla_\beta \frac{1}{R_{ab}} = \frac{3R_{ab}^\alpha R_{ab}^\beta - (R_{ab})^2 \delta_{\alpha\beta}}{(R_{ab})^5}, \quad (12)$$

where $R_{ab} = |\mathbf{R}_a - \mathbf{R}_b|$ denotes the distance between $\mathbf{R}_a$ and $\mathbf{R}_b$ and $\nabla_\alpha = \frac{\partial}{\partial R_{ab}^\alpha}$. Considering that $T_{ab}^{\alpha\gamma}$, $T_{ab}^{\beta\delta} \propto \frac{1}{R_{ab}^3}$, the dispersion energy, see Eq. (11), can be rewritten with the dipole–dipole dispersion coefficient $C_{6,ab}$ as

$$E_{disp,ab} = -\frac{C_{6,ab}}{R_{ab}^6}, \quad (13)$$

which gives the correct long-range behavior $\propto \frac{1}{R^6}$. As a result, the accuracy of the long-range dispersion term $E_{disp,ab}$ is largely determined by the accuracy of the $C_{6,ab}$ coefficients. Consequently, we are faced with the problem of how to evaluate C_6 for arbitrary

dispersion-bound systems from isolated atoms to molecules and extended systems.

2. Atom-pairwise corrections

Simplifying the problem to isotropic polarizabilities $\bar{\alpha}_a(i\omega), \bar{\alpha}_b(i\omega)$, the isotropic atom-pairwise $C_{6,ab}$ dispersion coefficient is given by the Casimir–Polder integral,[46]

$$C_{6,ab} = \frac{3}{\pi} \int_0^\infty \bar{\alpha}_a(i\omega) \bar{\alpha}_b(i\omega) \, d\omega. \tag{14}$$

Now, distributing a set of atoms $\{a\}$ to molecule A and atoms $\{b\}$ to molecule B, the dispersion energy $E_{\text{disp},AB}$ for molecules A, B can be given by the atom-pairwise dispersion energy of atom-pairwise $a \in A, b \in B$,[45]

$$E_{\text{disp},AB} = -\sum_{a,b} \frac{C_{6,ab}}{R_{ab}^6}, \tag{15}$$

leading to the pairwise additive description of the vdW interaction term $E_{\text{disp},AB}$, which gives the correct long-range behavior $\propto \frac{1}{R^6}$. However, it is important to remember that polarizabilities and dispersion coefficients within a molecule or a fragment can be highly anisotropic and are not simply the sum of the properties of the isolated atoms, which make up the molecule.[47] In fact, simply using free atom polarizabilities and dispersion coefficients would result in large errors for E_{disp}. This is because the polarizability of a given atom in a molecule is affected by its environment. Nonetheless, we can define effective polarizabilities $\bar{\alpha}_{a,\text{eff}}$, which take these environmental effects into account. With these, and effective atom-pairwise dispersion coefficients $C_{6,ab,\text{eff}}$, reliable E_{disp} can be recovered.[2] How $\bar{\alpha}_{a,\text{eff}}$ and/or $C_{6,ab,\text{eff}}$ are approximated differs between the atom-pairwise methods discussed below, each with its unique set of strengths and weaknesses.

a. Tkatchenko–Scheffler method. We start with the method developed by Tkatchenko and Scheffler (TS).[2] In order to avoid having to evaluate the frequency dependent polarizabilities $\bar{\alpha}(i\omega)$ in the Casimir–Polder integral [Eq. (14)] over all ω, $\bar{\alpha}(i\omega)$ is first expanded as a Padé series.[48] The leading term in this series is

$$\bar{\alpha}_a^1(w) = \frac{\bar{\alpha}_{a,\text{free}}}{1 - \left(\frac{\omega}{\eta_a}\right)^2} \tag{16}$$

with the effective frequency η_a. This leads to the London formula for $C_{6,ab}$,[49]

$$C_{6,ab} = \frac{3}{2}\left[\frac{\eta_A \eta_B}{\eta_A + \eta_B} \bar{\alpha}_{a,\text{free}} \bar{\alpha}_{b,\text{free}} \right], \tag{17}$$

using free-atom references for the polarizability $\bar{\alpha}_{a,\text{free}}, \bar{\alpha}_{b,\text{free}}$. $C_{6,ab}$ can then be rewritten in terms of homonuclear $C_{6,aa}, C_{6,bb}$ by using $\eta_a = \frac{4}{3} \frac{C_{6,aa}}{\bar{\alpha}_{a,\text{free}}^2}$ [derived from Eq. (17) for $a = b$],[2]

$$C_{6,ab} = \frac{2 C_{6,aa} C_{6,bb}}{\left[\frac{\alpha_{b,\text{free}}}{\alpha_{a,\text{free}}} C_{6,aa} + \frac{\alpha_{a,\text{free}}}{\alpha_{b,\text{free}}} C_{6,bb} \right]}. \tag{18}$$

As mentioned above, using free-atom references for $C_{6,aa}, C_{6,bb}$ does not accurately reflect the $C_{6,aa}, C_{6,bb}$ coefficients of atoms a, b within a molecule or a solid. Therefore, the TS method uses effective dispersion coefficients $C_{6,aa,\text{eff}}, C_{6,bb,\text{eff}}$, which are defined via the relationship between the polarizability and the atomic volume,[2,50] resulting in

$$C_{6,aa,\text{eff}} = \left(\frac{V_{a,\text{eff}}}{V_{a,\text{free}}} \right)^2 C_{6,aa,\text{free}} \tag{19}$$

with free-atom reference values $C_{6,aa,\text{free}}$.

The effective volume $V_{a,\text{eff}}$ of atom a in molecule A is obtained by the Hirshfeld partitioning of the density $n(\mathbf{r})$ with Hirshfeld weights $w_a(\mathbf{r})$,[2]

$$V_{a,\text{eff}} = \int r^3 w_a(\mathbf{r}) n(\mathbf{r}) d^3\mathbf{r}. \tag{20}$$

Importantly, TS was specifically designed to describe molecular vdW interactions but tends to overestimate them for metallic systems.[51] This can be attributed to several factors. First, semilocal GGA functionals already offer a reasonable description of the total energies and polarizabilities of metallic systems, as they reduce to LDA in regions of homogeneous electron density. Second, TS as an atom-in-molecule approach fails to account for screening effects and delocalized states in metallic systems, resulting in a significant overestimation of C_6 coefficients for bulk metals.[52] As a result, these combined effects lead to overestimated cohesive energies and underestimated lattice constants when combining TS with semilocal xc functionals for metallic systems.[51] For such cases, pairwise metal–metal TS dispersion contributions are usually excluded.[53] In addition, as Hirshfeld partitioning, see Eq. (20), uses neutral free atom references, errors for ionic materials are expected.[54] Iterative Hirshfeld partitioning[54] addresses this issue but is not widely available in electronic structure codes and complicates the calculation of analytical energy gradients.

b. Exchange-hole dipole moment. Similarly to TS, XDM[3,4,55] computes pairwise dispersion coefficients $C_{6,ab}^{\text{XDM}}$ based on the electrostatic interaction of the instantaneous dipoles on atoms a, b. Here, the source of these instantaneous dipoles is assumed to be the dipole moment of the corresponding exchange hole.[55,56] The dispersion coefficients $C_{6,ab}^{\text{XDM}}$ are then given by[55]

$$C_{6,ab}^{\text{XDM}} = \frac{\langle d_X^2 \rangle_a \langle d_X^2 \rangle_b \bar{\alpha}_{a,\text{eff}} \bar{\alpha}_{b,\text{eff}}}{\langle d_X^2 \rangle_a \bar{\alpha}_{b,\text{eff}} + \langle d_X^2 \rangle_b \bar{\alpha}_{a,\text{eff}}} \tag{21}$$

with the exchange-hole dipole moment $\langle d_{X\sigma}^2 \rangle$ given by[55]

$$\langle d_{X\sigma}^2 \rangle = \int \rho_\sigma(\mathbf{r}_1) d_{X\sigma}^2(\mathbf{r}_1) d^3\mathbf{r}_1. \tag{22}$$

$d_{X\sigma}^2$ is the magnitude of the dipole moments of the electron and its exchange hole squared. The polarizabilities $\bar{\alpha}_{a,\text{eff}}, \bar{\alpha}_{b,\text{eff}}$ are computed similarly to TS via Hirshfeld partitioning from free atomic densities and polarizabilities, leading to similar limitations for ionic materials. However, XDM can accurately describe molecular interactions

as well as covalent solids and metals.[4] For optimal performance of dispersion-corrected density functionals using the XDM method, Price *et al.* recommend using *dispersionless* exchange functionals, such as B86b.[52] In this context, the term dispersionless means imposing a constraint on the large gradient limit of the exchange enhancement factor $F_x(s)$,

$$\lim_{s \to \infty} F_x(s) \sim s^{2/5}. \tag{23}$$

This constraint makes the corresponding exchange functional highly repulsive.[52,57] In contrast, functionals that do not satisfy this constraint may mimic dispersion-like behavior in the short range, resulting in double counting of dispersion interactions and overbinding effects.[52] In practice, dispersionless functionals are excellent for systems dominated by non-covalent interactions (such as molecular crystals), but not necessarily good general-purpose methods for molecules, solids, and surfaces. Fortunately, overcounting effects can to a large extent be absorbed by appropriately parameterized damping functions (see below).

3. Many-body dispersion methods

Atom-pairwise methods can accurately predict long-range dipole–dipole dispersion interactions but neglect the anisotropy of atomic environments, screening, and many-body effects. Many-body dispersion methods such as MBD@rsSCS[5,20] and MBD-NL[6] address these shortcomings using a Random Phase Approximation (RPA) formalism and anisotropic polarizabilities.[58]

To this end, MBD@rsSCS and MBD-NL start from the uncoupled dipole description of QHOs and add many-body interactions by computing the energy of coupled QHOs using the MBD Hamiltonian. The MBD Hamiltonian for the interaction of N QHOs on atoms a with polarization weight displacement μ_a and the long-range dipole–dipole interaction tensor $\mathbf{T}_{ab}^{LR}$ is given by

$$H_{\text{MBD}} = -\sum_{a=1}^{N} \frac{1}{2} \nabla_{\mu_a}^2 + \sum_{a=1}^{N} \frac{1}{2} \omega_a^2 \mu_a^2 + \sum_{a>b}^{N} \omega_a \omega_b \sqrt{\alpha_a(0)\alpha_b(0)} \mu_a^+ \mathbf{T}_{ab}^{LR} \mu_b. \tag{24}$$

Diagonalizing the MBD Hamiltonian in the basis of QHOs gives modes with $3N$ squared eigenfrequencies $\lambda_i = \omega_i^2$. The MBD energy is then given by the zero-point energy difference of coupled QHOs and uncoupled QHOs,[5]

$$E_{\text{MBD}} = \frac{1}{2} \sum_{i=1}^{3N} \sqrt{\lambda_i} - \frac{3}{2} \sum_{a=1}^{N} \omega_a. \tag{25}$$

The MBD@rsSCS method builds on the TS dispersion correction. In particular, TS provides atom-pairwise isotropic atomic polarizabilities α_a^{TS} as starting points. To include the effects of short-range electrodynamic screening and anisotropy of chemical bonding on the polarizabilities, range-separated self-consistent screening (rsSCS) of the short-range atomic polarizabilities with the short-range dipole–dipole interaction tensor $T_{a,\text{SR}}$ is performed.[20] This involves solving a Dyson-like equation for each atom a, from which screened polarizabilities $\alpha_a^{\text{rsSCS}}(i\omega)$ and their screened characteristic frequencies ω_a are obtained self-consistently,[5]

$$\alpha_a^{\text{rsSCS}}(i\omega) = \alpha_{a,\text{SR}}^{\text{TS}}(i\omega) - \alpha_a^{\text{TS}}(i\omega) T_a \alpha_a^{\text{rsSCS}}(i\omega). \tag{26}$$

To ensure the convergence of these self-consistent equations, a robust electron density partitioning scheme for obtaining the input polarizabilities $\alpha_a^{\text{TS}}(i\omega)$ [see Eq. (20)] must be used. An inadequate partitioning into atomic fragments can lead to convergence issues of the rsSCS scheme or highly overestimated polarizabilities. This is, for example, observed for metallic systems with very delocalized electron densities.[6]

In contrast, MBD-NL uses the VV10 (Vydrov and van Voorhis) functional[40] to obtain atomic polarizabilities by averaging over $\alpha^{\text{VV}}[n](\mathbf{r}, \omega)$ for each atom a,

$$\alpha_a^{\text{VV}}(\omega) = \int w_a(\mathbf{r}) g(I, \chi) \alpha^{\text{VV}}[n](\mathbf{r}, \omega) \text{d}\mathbf{r}, \tag{27}$$

with Hirshfeld weights w_a, the local ionization potential I,[59] and the iso-orbital indicator function χ.[60] To avoid double counting, a cut-off function $g(I, \chi)$ from the SCAN functional is used.[6] The VV10 polarizability functional is an approximation that is geared toward solid systems and consequently does not reach the accuracy of high level reference polarizabilities for free atoms. To ensure a more accurate description, polarizabilities α_a^{rVV} are obtained by normalizing the ratio of $\alpha_a^{\text{VV,free}}$ to highly accurate free atom values $\alpha_a^{\text{ref,free}}$,[6]

$$\alpha_a^{\text{rVV}} = \alpha_a^{\text{VV}} \frac{\alpha_a^{\text{ref,free}}}{\alpha_a^{\text{VV,free}}}. \tag{28}$$

However, for highly polarized systems far from the free atom description, MBD-NL might still underestimate polarizabilities and consequently the dispersion interaction.

C. Damping functions

The dispersion energy of atom-pairwise methods $E_{\text{disp}} \propto \frac{-C_{6,ab}}{R_{ab}^6}$ [Eq. (15)] and many-body methods $E_{\text{disp}} \propto -\mathbf{T}_{ab} \cdot \mathbf{T}_{ab}$ [Eq. (11)] diverge in the short-range limit $R_{ab} \to 0$. To prevent this, and to adapt the dispersion correction to the underlying short-ranged xc functional, damping functions are employed. For pairwise corrections, these take the form

$$E_{\text{disp}} = -\sum_{n=6,8,10} \sum_{a,b} \frac{C_{n,ab}}{R_{ab}^n} f_{\text{damp}}(R_{ab}) \tag{29}$$

for the leading-order ($C_{6,ab}$) and higher-order ($C_{8,ab}$, $C_{10,ab}$, ...) terms.

The damping function f_{damp} interpolates E_{disp} between the asymptotic limits $E_{\text{disp}}(R_{ab} \to \infty) = -\sum_n \sum_{a,b} \frac{C_{n,ab}}{R_{ab}^n}$ and $E_{\text{disp}}(R_{ab} \to 0) = c$ with c being finite or zero. In the following, the damping functions used for the TS and XDM methods are introduced, although other variants exist.[61–63] These consist of the Wu–Yang (WY) and Becke–Johnson (BJ) functions, respectively. The WY function is a Fermi-type function given by[2,64]

$$f_{\text{damp}}^{\text{WJ}}(R_{ab}) = \frac{1}{1 + \exp\left[-d\left(\frac{R_{ab}}{s_R \cdot R_{\text{vdW},ab}} - 1\right)\right]} \tag{30}$$

with parameters d, s_R and pairwise reference vdW radii $R_{\text{vdW},ab}$. The BJ damping function is given by[65]

$$f_{\mathrm{damp},n}^{\mathrm{BJ}}(R_{ab}) = \frac{R_{ab}^n}{R_{ab}^n + (\alpha_1 \cdot R_{\mathrm{vdW},ab} + \alpha_2)^n} \qquad (31)$$

with parameters α_1, α_2 and pairwise reference vdW radii $R_{\mathrm{vdW},ab}$.

The role of f_{damp} is twofold. On the one hand, it ensures that the dispersion treatment does not cause singularities for small R_{ab}. On the other hand, it is crucial to ensure a reasonable description of systems going from the long-range dispersion interaction description to the short-range semilocal xc functional. This is essential because equilibrium geometries of dispersion-bound systems are often situated in the intermediate range. Therefore, the parameterization of f_{damp} has to be adjusted to the used xc functional, although not all parameters are necessarily functional-dependent. For example, the damping strength d of the WY damping function has been shown to have a robust performance for fixed $d = 20$ regardless of the underlying functional.[66] In contrast, the onset of the damping (determined by s_R for the WY damping function and by α_1 and α_2 for the BJ damping function) is highly functional dependent and consequently has to be adjusted for each xc functional separately.

Similarly, the divergence of the many-body MBD@rsSCS and MBD-NL methods is prevented by range-separating the short- ($\mathbf{T}_{\mathrm{SR}}$) and long-range ($\mathbf{T}_{\mathrm{LR}}$) components of the dipole–dipole interaction tensor $\mathbf{T}$,

$$\mathbf{T}_{\mathrm{SR}} = (1 - f_{\mathrm{range}}(R_{ab}))\mathbf{T} \qquad (32)$$

and

$$\mathbf{T}_{\mathrm{LR}} = \mathbf{T} - \mathbf{T}_{\mathrm{SR}}. \qquad (33)$$

For f_{range}, a modified WY damping function with damping strength $d = 6$ is used.[20] Note that the functional-specific parameter β for the MBD methods corresponds to the parameter s_R in Eq. (30).

D. Parameterization

Each of the atom-pairwise and many-body dispersion treatments considered in this work (TS, XDM, MBD@rsSCS, and MBD-NL) uses different approximations to describe dispersion interactions and different empirical damping functions f_{damp}. Now, we aim to adequately parameterize these corrections for use with the semilocal BEEF xc functional. To facilitate a fair comparison between the methods, we fit the functional specific parameters for the dispersion correction methods on the same dataset and loss function. The dataset we use as a reference is the S22 dataset[67] of CCSD(T)/CBS extrapolated interaction energies from Takatani et al.,[68] which is routinely used to fit and benchmark methods for noncovalent interactions. In particular, S22 was also used as a part of the parameterization procedure of the BEEF-vdW(DF2) functional so that using this dataset ensures consistency with the original functional.

The loss function for the parameterization was determined as the root mean square error (RMSE) of the S22 dataset,

$$RMSE = \sqrt{\frac{1}{N}\sum_{i=1}^{N}\left(E_{\mathrm{BEEF-vdW(disp)}} - E_{\mathrm{CCSD(T)/CBS}}\right)^2}. \qquad (34)$$

The xc specific parameters for each correction were optimized with the Nelder–Mead algorithm.[69,70] The resulting parameters can be found in Table I.

TABLE I. Fitted functional dependent parameters of TS, MBD@rsSCS, MBD-NL, and XDM for use with the BEEF xc functional. Constrained optimization was used for XDM to ensure that the van der Waals radii in the BJ damping $R_{\mathrm{vdW},ab}$ remain physically meaningful, i.e., $R_{\mathrm{vdW},ab} > 0$. For details, see the supplementary material.

vdW treatment	Fitted functional dependent parameters
TS	$s_R = 0.6038$
MBD@rsSCS	$\beta = 0.5522$
MBD-NL	$\beta = 0.5927$
XDM	$a_1 = 1.6217$, $a_2 = -1.6217$

This reveals that the damping functions result in relatively short-ranged onsets of the correction. For example, the TS function has $s_R = 0.6038$. For similarly repulsive surface-science functionals such as revPBE or RPBE, comparable parameters are found [$s_R(\mathrm{RPBE}) = 0.590$, $s_R(\mathrm{revPBE}) = 0.585$].[71] In the literature, such short onsets of the dispersion correction are attributed to non-dispersionless xc functionals, which might impact the performance of the semiempirical dispersion correction and result in the over-stabilization of hydrogen bonding and the understabilization of dispersion-bound systems for some types of dispersion corrections.[52] However, we note that the BEEF xc functional was originally developed with the use of the nonlocal vdW-DF2 functional in mind. Without vdW-DF2, the short-range correlation contributions from vdW-DF2 will also be absent. This is bound to impact the short-range behavior of the overall xc energy. Therefore, it is not surprising that additive dispersion corrections might try to compensate for this effect by using a short onset of the correction.

Note that while the choice to parameterize the damping function to non-covalent molecular dimers is the most commonly used approach, in principle other properties (such as chemisorption energies, see below) could also be used for fitting. This would clearly improve the results for these properties, but it has the danger of producing a method that is right for the wrong reason (e.g., by partially attributing covalent interactions to dispersion). In general, this would lead to a less transferable method and can have unforeseen detrimental consequences for other properties.

E. Computational details

BEEF-vdW(disp) computations with TS, MBD@rsSCS, MBD-NL, and XDM were performed using the electronic structure code FHI-aims[72] (version 221103) with *tight* numeric atomic orbital (NAO) basis and integration settings on an HPC cluster with Intel Xeon Cascade Lake-AP processors (Xeon Platinum 9242). FHI-aims uses an all-electron approach, treating core and valence electrons explicitly, facilitating a consistent treatment of lighter and heavier elements. Relativistic effects are included with the atomic scalar zeroth-order approximation.[73] For all computations using the TS dispersion correction, metal–metal interactions were excluded. The self-consistency convergence criteria for non-spin polarized computations were set to 1×10^{-5} eV (total energy), 1×10^{-3} eV (sum of eigenvalues), 1×10^{-4} e/Å^3 (charge density), and 1×10^{-3} eV/Å (forces). For structure relaxations, forces were relaxed below 5×10^{-2} eV/Å. Figure S1 shows the convergence of cohesive energy for both spin-polarized and non-spin-polarized relaxations, confirming proper convergence of the computed observables.

FHI-aims employs the BEEF xc functional as implemented in libxc.[74] The corresponding keyword in FHI-aims is: xc libxc GGA_XC_BEEFVDW. In addition, the keywords atomic_solver sratom and atomic_solver_xc pw-lda were employed. Although FHI-aims supports computations with the vdW-DF2 functional, its implementation does not make use of the FFT approach demonstrated later by Román-Pérez and Soler et al.[18] and is therefore not practical for larger molecular and bulk structures. Consequently (and to ensure consistency with the literature), all reference values for BEEF-vdW(DF2) are taken from Ref. 12.

III. RESULTS AND DISCUSSION

Having parameterized the atom-pairwise and many-body dispersion corrections for use with the semilocal BEEF xc functional, we test the performance of these methods for a range of molecular, solid, and surface systems, for which the original BEEF-vdW(DF2) functional was designed. In particular, we examine the performance for noncovalent molecular systems (S22x5[75] and S66x10[63,76,77]), solids (Sol27Ec[12] and Sol27Lc[12]), and chemisorption of adsorbates on metal surfaces (CE27[12]).

A. Noncovalent, intermolecular interactions

First, we examine the performance of the BEEF-vdW variants for the interaction energies of the S22 dataset,[67] compared to the CCSD(T)/CBS extrapolated interaction energies from Takatani et al.;[68] see Fig. 2(a). The reference method BEEF-vdW(DF2) underestimates the interaction energies[12] compared to CCSD(T)/CBS. This underestimation is in part due to the generally repulsive nature of the BEEF xc functional. In fact, exchange functionals with similarly steeply rising exchange enhancement factors, such as revPBE, also exhibit underestimated interaction energies for the S22 dataset when combined with nonlocal vdW-DF functionals.[12,33,38]

Furthermore, vdW-DF2 is just a reparameterized version of vdW-DF1, which has shown deficiencies for molecule–molecule interactions that cannot be fully remedied by a simple reparameterization.[33,35,38]

All atom-pairwise and many-body dispersion corrections improve the accuracy of the interaction energies compared to BEEF-vdW(DF2) on average. In particular, the pairwise XDM and TS methods obtain highly accurate interaction energies for the S22 dataset. In contrast, MBD@rsSCS and MBD-NL exhibit slightly higher errors compared to the atom-pairwise corrections. Examining the performance of the MBD methods for functionals of similar repulsiveness, such as RPBE and revPBE, we notice a comparable level of errors for the S22 dataset (see the supplementary material). In contrast, less repulsive functionals, such as PBE and PBE0, have demonstrated very good performance for the S22 dataset with these corrections.[5,20] This suggests that the underestimation of the interaction energies stems mainly from the repulsive nature of the BEEF functional rather than from the shortcomings of the MBD@rsSCS and MBD-NL methods.

The S22 dataset can be classified by bonding type into predominantly hydrogen-bonded, dispersion-bound, and "mixed" complexes. We examine the performance of the dispersion treatments for each bonding category in Fig. 2(b). Unsurprisingly, the plain BEEF xc functional (without dispersion corrections) exhibits the largest mean absolute relative error (MARE) for all bonding categories. It is least effective when describing dispersion-bound systems and performs best for hydrogen-bonded systems, which are predominantly bound by classical electrostatic interactions. When using the dispersion corrected BEEF-vdW variants, the errors across all bonding categories are reduced. Nonetheless, the performance of the dispersion corrected methods is strongly influenced by the character of the underlying BEEF xc functional, with identical ordering of relative errors for H-bonds, mixed and dispersion bound systems. Examining the performance of the reference BEEF-vdW(DF2)
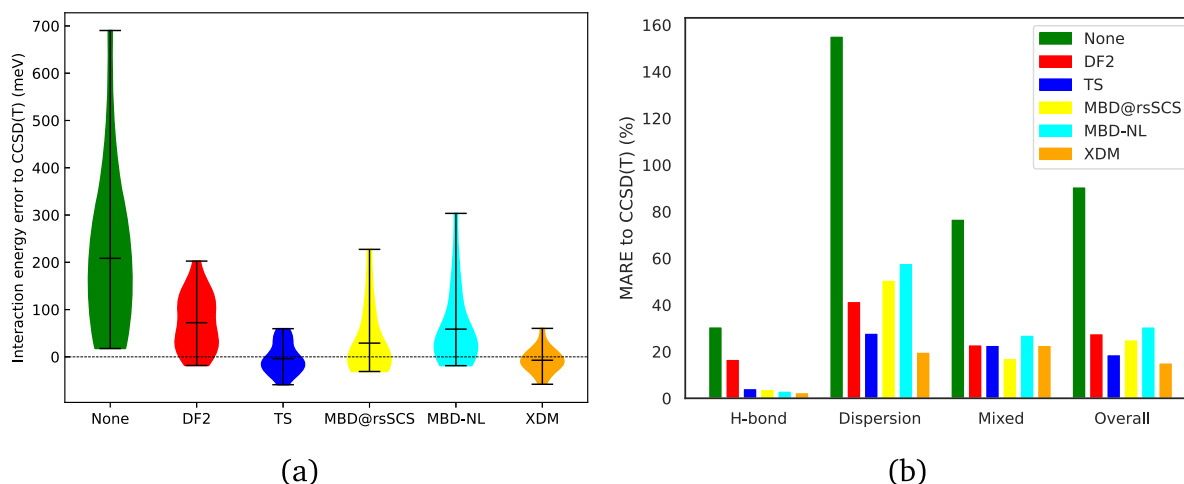

FIG. 2. Performance of BEEF-vdW(disp) with TS, MBD@rsSCS, MBD-NL, and XDM compared to the uncorrected, plain BEEF-vdW(none), and the original BEEF-vdW(DF2) functional for the S22 dataset. Reference values are CCSD(T)/CBS interaction energies.[68] (a) Interaction energy error distributions. The mean and extrema are shown by black lines. (b) Mean absolute relative interaction energy error categorized for predominantly hydrogen, dispersion, and "mixed" bonded complexes. BEEF-vdW(DF2) interaction energies are from Ref. 12. CCSD(T)/CBS interaction energies are from Ref. 68.

method, it exhibits comparatively high errors across all bonding categories and especially for hydrogen-bonded systems, where it performs significantly worse than the other variants. Indeed, BEEF-vdW(DF2) is known to perform worse compared to vdW-DF1 (vdW-DF1-revPBE) and vdW-DF2 (vdW-DF1-PW86R) for the S22 dataset.[78] Overall, the atom-pairwise TS and XDM methods show the highest accuracy for all interactions, while the many-body dispersion methods MBD@rsSCS and MBD-NL tend to underestimate the interaction energies to a similar degree as BEEF-vdW(DF2).

The S22 dataset consists of 22 equilibrium geometries of small molecular dimers. In practice, dispersion corrected DFT methods are used to study complex systems, for which equilibrium as well as non-equilibrium interactions of differently sized systems and molecular fragments have to be adequately described. To explore this regime, we next examine the performance of the BEEF-vdW variants for the S22x5[75] and S66x10[63,76,77] datasets, which are common benchmark sets for noncovalent interactions. S22x5 includes four additional non-equilibrium configurations for each S22 dimer structure at 0.9, 1.2, 1.5, and 2.0 times the equilibrium distance. S66x10 includes 660 configurations of 66 molecular dimers (partially overlapping with S22) at ten intermolecular distances (at 0.7, 0.8, 0.9, 0.95, 1.0, 1.05, 1.1, 1.25, 1.5, and 2.0 times the equilibrium distance). Compared to S22, S66 offers a larger variety of dimers for each bonding category.

First, we analyze how the mean absolute interaction energy error changes with intermolecular separation between molecules for S22x5 in Fig. 3(a). For the underlying BEEF xc functional, the error increases with decreasing intermolecular distance. This effect stems from the missing attractive dispersion contributions, the overly repulsive nature of the BEEF functional, as well as from discrepancies between the BEEF and CCSD(T) description of the electrostatic contributions. BEEF-vdW(DF2) decreases the MAE compared to not using any dispersion treatment but still follows the tendency of

BEEF-vdW(none) to be overly repulsive at short distances. Comparing the atom-pairwise and many-body methods, the latter show a similar performance to DF2, whereas TS and XDM have on average the smallest errors over all interaction distances. However, the many-body methods outperform the atom-pairwise methods TS and XDM for larger intermolecular separations.

We further investigated how effective the atom-pairwise and many-body dispersion corrections are in treating molecular systems of increasing size; see Fig. 3(b). The error of the underlying BEEF functional without dispersion treatment increases for increasing system size, because the dispersion interaction energy is size extensive. The TS method effectively decreases the error but increasingly overcorrects with increasing system size. This limited transferability to the S66 dataset might be a result of overfitting on the S22 dataset. In contrast, both examined MBD methods (yellow and cyan) do not display such a systematic overestimation, although they display some outliers where the dispersion energy is underestimated. Finally, the XDM method (orange) shows an effective correction to a constant error regardless of system sizes, even though the method on average overcorrects slightly across the full range of systems.

This is further corroborated by considering the performance on the L7 dataset (see Fig. S7).[79] L7 consists of large molecular complexes, based on binding patterns found in supramolecular biological systems, containing dispersion and hydrogen-bonded systems. All employed dispersion corrections improve the description of these interactions compared to the uncorrected, plain BEEF-vdW(none) functional. Consistent with the analysis of the S22 and S66 sets, we find that TS has a slight tendency toward overbinding for these large systems, while the many-body dispersion corrections tend to underbind. XDM again emerges as the most accurate method.

To further test the transferability of the parameters, we furthermore assessed the performance of the new BEEF-vdW variants on
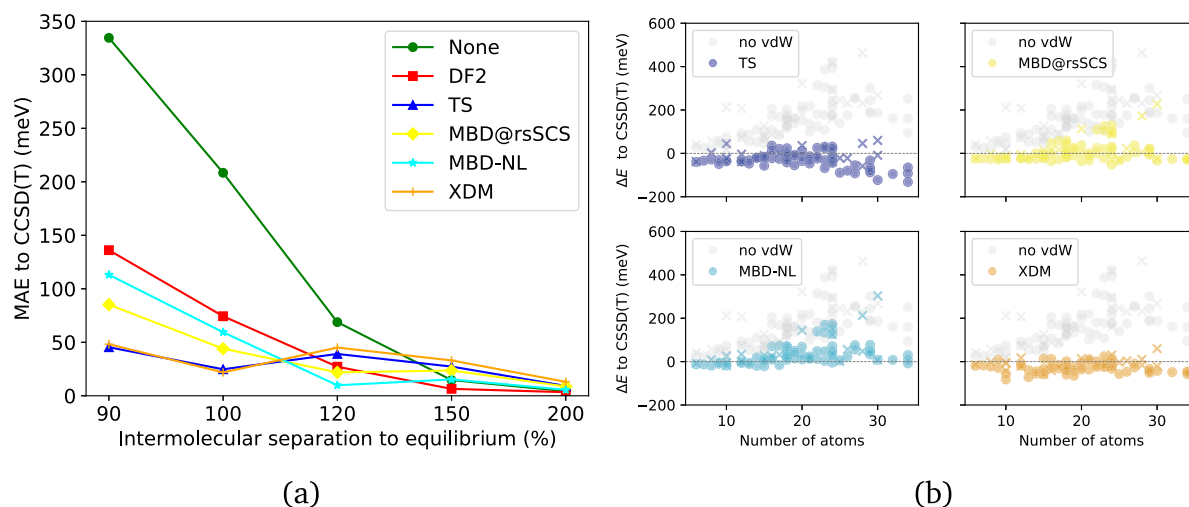

(a)

(b)

FIG. 3. Performance of BEEF-vdW(disp) with TS, MBD@rsSCS, MBD-NL, and XDM compared to the plain, uncorrected BEEF-vdW(none) and the original BEEF-vdW(DF2)[12] functional for CCSD(T)/CBS interaction energies[68] for (a) nonequilibrium intermolecular separations of the S22x5 dataset and (b) with the system size for the S22x5 1.0 (crosses) and S66x10 1.0 (dots) datasets. BEEF-vdW(DF2) interaction energies are from Ref. 12.

the NCIA250 dataset,[80] which was designed to represent the worst-performing cases within the D1200, HB375, HB300SPX, SH250, and R739 datasets of non-covalent molecular interactions (2846 data points) in a concise way with only 250 systems. The performance of BEEF-vdW(disp) variants largely aligns with the performance observed for the S22 and S66 datasets. Indeed, the RMSEs for NCIA250 are comparable to or lower than those for S22; see Fig. S8. This confirms that the parameterizations presented herein are transferable to more complex non-covalent bonding situations. Indeed, it is notable that the many-body dispersion methods such as BEEF-vdW(MBD@rsSCS) and BEEF-vdW(MBD-NL) perform significantly better compared to the S22 dataset and are on par with the atom-pairwise methods here.

B. Cohesive energies and lattice constants

The good performance of the new BEEF-vdW variants for molecular dimers relative to the original BEEF-vdW(DF2) method is encouraging. However, dispersion corrections are generally parameterized for exactly these interactions so that good performance is expected. For a general-purpose method, this should not come at the cost of lower performance for the properties of bulk solids. To verify this, we used the Sol27Ec and Sol27Lc datasets,[12] which contain lattice constants (a_0) and cohesive energies (E_{coh}) of 27 crystalline systems, namely Li(bcc), Na(bcc), K(bcc), Rb(bcc), Ca(fcc), Sr(fcc), Ba(bcc), V(Bcc), Nb(bcc), Ta(bcc), Mo(bcc), W(bcc), Fe(bcc), Rh(fcc), Ir(fcc), Ni(fcc), Pd(fcc), Pt(fcc), Cu(fcc), Ag(fcc), Au(fcc), Al(fcc), Pb(fcc), C(dia), Si(dia), Ge(dia), and Sn(dia). The experimental reference values for E_{coh} and a_0 from Ref. [12] are zero-point vibrational energy (ZPVE) and zero-point anharmonic expansion (ZPAE) corrected to enable the comparison of computational results with experiment. The cohesive energy E_{coh} is computed from the energy of the free atom E_{atom} and the energy of the bulk solid E_{bulk} with N_{bulk} atoms,

$$E_{coh} = E_{atom} - \frac{E_{bulk}}{N_{bulk}}. \quad (35)$$

The performance of the BEEF-vdW variants for the Sol27 dataset is shown in Fig. 4. The reference method BEEF-vdW(DF2) underestimates cohesive energies (note that by definition $E_{coh} > 0$) and overestimates lattice constants compared to the experimental reference values. This is a known behavior for vdW-DF used with xc functionals that display steeply rising exchange enhancement factors.[33] Indeed, other functionals commonly used in surface science (such as revPBE and RPBE) are also known to overestimate lattice constants.[24] Unsurprisingly, the uncorrected BEEF-vdW(none) shows an even stronger underbinding behavior.

The TS method was not designed to account for screening effects and delocalized states needed to describe metallic systems, leading to large overbinding effects for pairwise metal–metal interactions. Therefore, in practice, pairwise metal–metal interactions are usually excluded for the TS method. Consequently, BEEF-vdW(TS) is identical to BEEF-vdw(none) for the metals in the dataset but shows improved results for covalently bound solids (see the supplementary material). On average, this results in a slight improvement in BEEF-vdW(TS) over BEEF-vdW(none), but worse performance than the original BEEF-vdW(DF2) method. MBD@rsSCS can, in principle, improve the description of metallic systems compared to TS, as it models many-body effects as well as gives a more realistic description of atomic polarizabilities due to the self-consistent rsSCS scheme. However, MBD@rsSCS shows strong overbinding for metals because the atomic partitioning of the polarizability fails to accurately represent the inherently delocalized nature of metallic systems.[81] For the Sol27Ec and Sol27Lc datasets, this leads to strongly overestimated polarizabilities for the metals and/or negative eigenvalues for the MBD Hamiltonian. Therefore, we could not obtain cohesive energies and lattice constants for
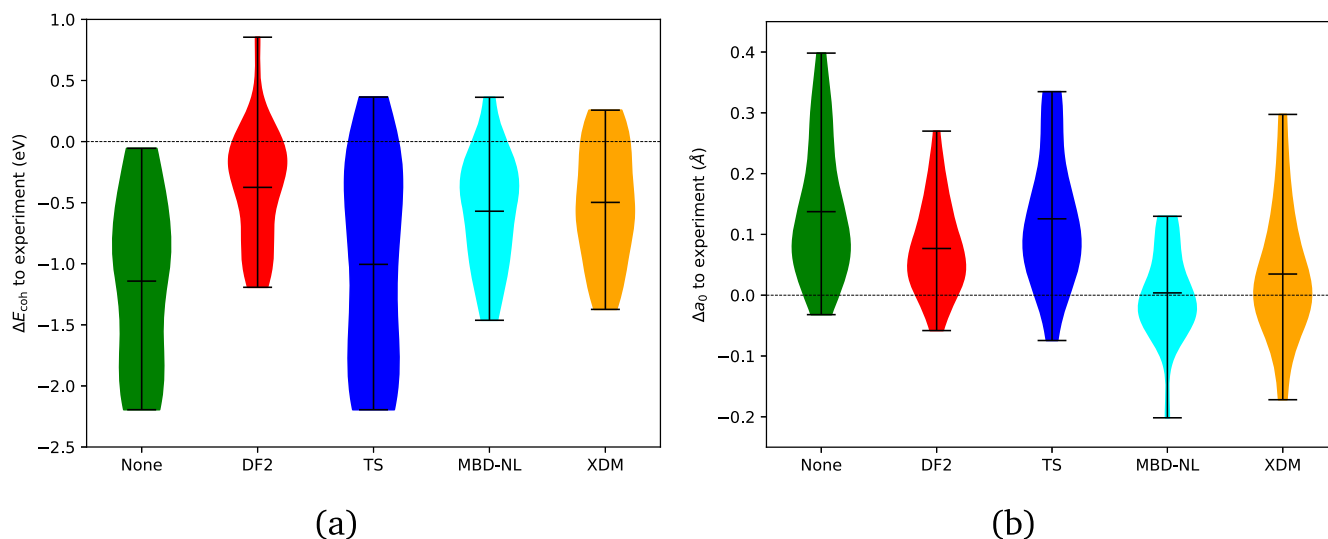

FIG. 4. Performance of BEEF-vdW(disp) with TS (metal–metal interaction terms excluded), MBD-NL, XDM compared to the plain, uncorrected BEEF-vdW(none) and the original BEEF-vdW(DF2)[12] functional for the Sol27[12] dataset. (a) Cohesive energy deviation to experiment. (b) Lattice constant deviation to experiment. Cohesive energies and lattice constants for BEEF-vdW(DF2) are from Ref. [12]. The mean and extrema are shown by black lines.

the full Sol27 dataset using the MBD@rsSCS method. However, BEEF-vdW(MBD@rsSCS) does yield accurate lattice constants and cohesive energies for the non-metallic systems within Sol27 (C, Si, Ge); see the supplementary material.

Dispersion corrections that are able to handle the delocalized nature of metallic electrons more effectively, such as XDM and MBD-NL, obtain reasonable, albeit slightly underbound, cohesive energies for the Sol27 dataset. XDM's robust performance results in better cohesive energies compared to BEEF-vdW(TS), although it cannot quite reach the accuracy of the original BEEF-vdW(DF2). Lattice constants obtained with BEEF-vdW(XDM) show an improved mean error compared to BEEF-vdW(TS) and BEEF-vdW(DF2) but also exhibit a relatively wide spread of errors. BEEF-vdW(MBD-NL) shows good overall performance for all examined bulk materials and obtains the most accurate lattice constants of all examined methods. In summary, the examined covalently bound and metallic systems are severely underbound by the BEEF xc functional, which is also reflected in the performance of the dispersion corrected BEEF-vdW variants. Due to significantly overestimated polarizabilities resulting in negative eigenvalues from the diagonalization of the MBD Hamiltonian, the use of MBD@rsSCS for metallic systems is not advisable. Overall, BEEF-vdW(MBD-NL) shows the best performance in obtaining cohesive energies and lattice constants for the Sol27 dataset, closely followed by the XDM method.

C. Molecular chemisorption on metallic surfaces

One of the main areas of application of the BEEF-vdW functional is in heterogeneous catalysis. This is notoriously challenging for semilocal functionals, as it requires simultaneously describing extended (metallic) catalyst surfaces, molecular adsorbates, and their mutual interactions. In this section, we examine the performance of the new BEEF-vdW variants for describing molecular chemisorption on metallic surfaces. BEEF-vdW(DF2) was specifically designed for this task, with the CE17 chemisorption dataset featuring prominently in the loss function.[12] Herein, we consider the broader CE27 chemisorption dataset, of which CE17 is a subset (see Fig. 5). These benchmarks encompass chemisorption energies of small molecules on late transition metal surfaces at low coverages.[12] Here, the chemisorption energy ΔE_c is defined as

$$\Delta E_c = E_{AM} - E_M - E_A, \qquad (36)$$

with E_A, E_M, and E_{AM} being the energies of the adsorbate, the metallic surface, and the combined system, respectively. To obtain the chemisorption energies, adsorbates, surfaces, and combined systems were relaxed with each of the examined methods (see the supplementary material for details). Chemisorption energies involving oxygen $\Delta E_c(O)$ were evaluated as described in Ref. 12 as $\Delta E_c(O) = \frac{1}{2}(\Delta E_c(O_2) - E_b(O_2))$ with $\Delta E_c(O_2)$ computed using Eq. (36) and the dioxygen bond energy $E_b(O_2) = 5.11$ eV from Ref. 82.

Above, we have observed that the uncorrected BEEF-vdW(none) underbinds both non-covalent and bulk systems. Therefore, it is not surprising that the chemisorption energies obtained with BEEF-vdW(none) are underbound as well. Meanwhile, the original BEEF-vdW(DF2) model performs best for this benchmark,
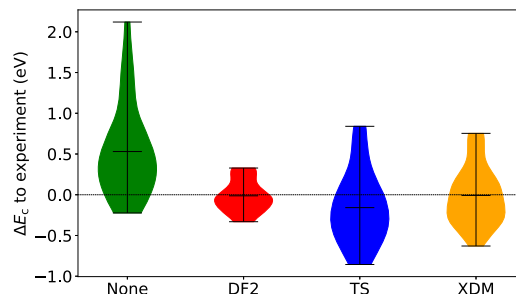

FIG. 5. Performance of BEEF-vdW(disp) with TS (metal–metal interactions excluded) and XDM compared to the plain, uncorrected BEEF-vdW(none) and the original BEEF-vdW(DF2) functional for the CE27 dataset regarding the chemisorption energy deviation to experiment. Chemisorption energies obtained with BEEF-vdW(DF2) are from Ref. 12. The mean and extrema are shown by black lines.

as might be expected given its specialized parameterization. Unfortunately, the many-body methods considered above could not be applied here. While the limitations of MBD@rsSCS for metals were already discussed (and are well known), MBD-NL also proved to be numerically unstable in some of the cases (as reflected in the negative eigenvalues of the MBD Hamiltonian). This can be attributed to the inadequacy of free atom references for the polarizabilities when describing metal surfaces.[51] Indeed, when using screened reference polarizabilities and C_6 coefficients from the vdW^{surf} method, the MBD-NL calculations could be performed. However, these screened parameters are only available for few elements (Ni, Cu, Zn, Pd, Ag, Pt, and Au) and have not been widely tested with MBD-NL. Nevertheless, this points to the fact that a robust MBD-NL-based surface science functional can be developed.

In contrast, the simpler atom-pairwise methods (TS and XDM) already yield reasonable results in all cases, although significant deviations (above 0.5 eV in some cases) were observed for both methods. Nevertheless, XDM in particular is a robust and computationally efficient alternative for describing chemisorption with the BEEF functional. The excellent performance of BEEF-vdW(DF2) underscores the advantage of specifically designing an xc functional with a given dispersion correction in mind, as was, for example, also done for the B97-D functional and the 3c methods developed by Grimme for molecular systems.[66,83] A bespoke surface-science oriented functional based on XDM would thus likely display an even better performance.

IV. CONCLUSION

To increase the general applicability of the BEEF-vdW functional for surface science applications, the performance of alternative BEEF-vdW variants using computationally efficient atom-pairwise and many-body dispersion treatments was explored. The atom-pairwise TS method shows robust performance for all non-covalent interactions investigated, with particularly good performance for molecular dimers, although a slight overcorrection for larger systems is observed. When metal–metal dispersion interactions are neglected, BEEF-vdW(TS) provides an overall robust method for the description of solids and chemisorption. However, it does not reach the accuracy of the original BEEF-vdW(DF2)

27 February 2025 08:49:16

method. The atom-pairwise XDM method shows well-rounded behavior for all examined systems. For molecular systems, XDM's performance is similar to that of TS with the difference that it shows no signs of deterioration for larger molecular dimers. In contrast to TS, XDM significantly improves the prediction of solid-state properties and chemisorption energies. Overall, the BEEF-vdW(XDM) method thus can be recommended as a general-purpose functional, with comparable and, for molecular systems, somewhat better accuracy than BEEF-vdW(DF2). Importantly, the uncertainty estimates from BEEF-vdW, intrinsic to the underlying semilocal functional, remain applicable to the BEEF-vdW(XDM) variant.

The many-body MBD@rsSCS and MBD-NL methods show a reliable performance for molecular dimers, comparable to BEEF-vdW(DF2), but are outperformed by TS and XDM. This is mostly due to the repulsive nature of the underlying BEEF xc functional. The simpler atom-pairwise methods seem to be better able to adjust to these issues, with appropriately parameterized damping functions. Unfortunately, MBD@rsSCS is not applicable for metallic systems and adsorbate-metal systems, because the atomic partitioning of the polarizability does not accurately capture the inherently delocalized nature of metallic systems. This results in significantly overestimated polarizabilities and/or negative eigenvalues for the MBD Hamiltonian. As a result, it is overall not advisable to use MBD@rsSCS with the BEEF xc functional. In contrast, MBD-NL is significantly more reliable, performing best for the Sol27 dataset. Unfortunately, MBD-NL also displayed numerical issues for certain chemisorbed systems so that it could not be rigorously evaluated in this context.

Based on the presented results, the pairwise XDM correction can be recommended as a cost-efficient drop-in replacement for the DF2 method in the BEEF-vdW functional, when the use of the latter is computationally inconvenient. Indeed, BEEF-vdW(XDM) is actually an improvement over the original for molecular systems. As mentioned above, the XDM method is often used in combination with dispersionless exchange functionals (such as B86b) for molecular applications. These are defined via an exact condition for the large-gradient limit of the exchange enhancement factor. This condition is incompatible with the local Lieb–Oxford bound that is (at least approximately) obeyed by surface science and condensed matter functionals such as PBE, RPBE, and BEEF.[9] In this sense, BEEF-vdW(XDM) can be considered to be complementary to these functionals. More broadly, the current work indicates that developing new functionals in the spirit of BEEF-vdW based on XDM would be highly promising. If the remaining numerical issues can be overcome, the MBD-NL method would also be highly promising for such a development, since it shows the best performance for solids and is known to be highly accurate for molecules, when combined with an appropriate xc functional.

SUPPLEMENTARY MATERIAL

The supplementary material encompasses additional computational details and analysis.

ACKNOWLEDGMENTS

AUTHOR DECLARATIONS

Conflict of Interest

The authors have no conflicts to disclose.

Author Contributions

Elisabeth Keller: Conceptualization (equal); Data curation (equal); Formal analysis (equal); Methodology (equal); Software (equal); Visualization (equal); Writing – original draft (equal). **Volker Blum**: Supervision (equal); Writing – review & editing (equal). **Karsten Reuter**: Supervision (equal); Writing – review & editing (equal). **Johannes T. Margraf**: Conceptualization (equal); Formal analysis (equal); Funding acquisition (equal); Methodology (equal); Supervision (equal); Writing – review & editing (equal).

DATA AVAILABILITY

The data that support the findings of this study are available within the article and its supplementary material.

REFERENCES

[1] S. Grimme, J. Antony, S. Ehrlich, and H. Krieg, "A consistent and accurate *ab initio* parametrization of density functional dispersion correction (DFT-D) for the 94 elements H-Pu," J. Chem. Phys. **132**, 154104 (2010).

[2] A. Tkatchenko and M. Scheffler, "Accurate molecular van der Waals interactions from ground-state electron density and free-atom reference data," Phys. Rev. Lett. **102**, 073005 (2009).

[3] A. D. Becke and E. R. Johnson, "Exchange-hole dipole moment and the dispersion interaction revisited," J. Chem. Phys. **127**, 154108 (2007).

[4] A. Otero-de-la Roza and E. R. Johnson, "Van der Waals interactions in solids using the exchange-hole dipole moment model," J. Chem. Phys. **136**, 174109 (2012).

[5] A. Tkatchenko, R. A. DiStasio, R. Car, and M. Scheffler, "Accurate and efficient method for many-body van der Waals Interactions," Phys. Rev. Lett. **108**, 236402 (2012).

[6] J. Hermann and A. Tkatchenko, "Density functional model for van der Waals interactions: unifying many-body atomic approaches with nonlocal functionals," Phys. Rev. Lett. **124**, 146401 (2020); arXiv:1910.03073 [cond-mat, physics:physics].

[7] H. Rydberg, B. I. Lundqvist, D. C. Langreth, and M. Dion, "Tractable nonlocal correlation density functionals for flat surfaces and slabs," Phys. Rev. B **62**, 6997–7006 (2000).

[8] H. Rydberg, M. Dion, N. Jacobson, E. Schröder, P. Hyldgaard, S. I. Simak, D. C. Langreth, and B. I. Lundqvist, "Van der Waals density functional for layered structures," Phys. Rev. Lett. **91**, 126402 (2003).

[9] M. Dion, H. Rydberg, E. Schröder, D. C. Langreth, and B. I. Lundqvist, "Van der Waals density functional for general geometries," Phys. Rev. Lett. **92**, 246401 (2004).

[10] K. Lee, É. D. Murray, L. Kong, B. I. Lundqvist, and D. C. Langreth, "Higher-accuracy van der Waals density functional," Phys. Rev. B **82**, 081101 (2010).

[11] O. A. Vydrov and T. Van Voorhis, "Benchmark assessment of the accuracy of several van der Waals density functionals," J. Chem. Theory Comput. **8**, 1929–1934 (2012).

[12] J. Wellendorff, K. T. Lundgaard, A. Møgelhøj, V. Petzold, D. D. Landis, J. K. Nørskov, T. Bligaard, and K. W. Jacobsen, "Density functionals for surface science:

Exchange-correlation model development with Bayesian error estimation," Phys. Rev. B **85**, 235149 (2012).

[13] A. Bruix, J. T. Margraf, M. Andersen, and K. Reuter, "First-principles-based multiscale modelling of heterogeneous catalysis," Nat. Catal. **2**, 659–670 (2019).

[14] B. Kreitz, P. Lott, F. Studt, A. J. Medford, O. Deutschmann, and C. F. Goldsmith, "Automated generation of microkinetics for heterogeneously catalyzed reactions considering correlated uncertainties," Angew. Chem., Int. Ed. **62**, e202306514 (2023).

[15] A. J. Medford, A. Wellendorff, A. Vojvodic, F. Studt, F. Abild-Pedersen, K. W. Jacobsen, T. Bligaard, and J. K. Nørskov, "Assessing the reliability of calculated catalytic ammonia synthesis rates," Science **345**, 197–200 (2014).

[16] Z. W. Ulissi, A. J. Medford, T. Bligaard, and J. K. Nørskov, "To address surface reaction network complexity using scaling relations machine learning and DFT calculations," Nat. Commun. **8**, 14621 (2017).

[17] K. Berland, V. R. Cooper, K. Lee, E. Schröder, T. Thonhauser, P. Hyldgaard, and B. I. Lundqvist, "van der Waals forces in density functional theory: A review of the vdW-DF method," Rep. Prog. Phys. **78**, 066501 (2015).

[18] G. Román-Pérez and J. M. Soler, "Efficient Implementation of a van der Waals density functional: Application to double-wall carbon nanotubes," Phys. Rev. Lett. **103**, 096102 (2009).

[19] E. Caldeweyher, C. Bannwarth, and S. Grimme, "Extension of the D3 dispersion coefficient model," J. Chem. Phys. **147**, 034112 (2017).

[20] A. Ambrosetti, A. M. Reilly, R. A. DiStasio, and A. Tkatchenko, "Long-range correlation energy calculated from coupled atomic response functions," J. Chem. Phys. **140**, 18A508 (2014).

[21] J. J. Mortensen, K. Kaasbjerg, S. L. Frederiksen, J. K. Norskov, J. P. Sethna, and K. W. Jacobsen, "Bayesian error estimation in density-functional theory," Phys. Rev. Lett. **95**, 216401 (2005); arXiv:cond-mat/0506225.

[22] J. P. Perdew and Y. Wang, "Accurate and simple analytic representation of the electron-gas correlation energy," Phys. Rev. B **45**, 13244–13249 (1992).

[23] J. P. Perdew, K. Burke, and Y. Wang, "Generalized gradient approximation for the exchange-correlation hole of a many-electron system," Phys. Rev. B **54**, 16533–16539 (1996).

[24] B. Hammer, L. B. Hansen, and J. K. Nørskov, "Improved adsorption energetics within density-functional theory using revised Perdew-Burke-Ernzerhof functionals," Phys. Rev. B **59**, 7413–7421 (1999).

[25] Y. Zhang and W. Yang, "Comment on 'Generalized gradient approximation made simple'," Phys. Rev. Lett. **80**, 890 (1998).

[26] J. P. Perdew, A. Ruzsinszky, G. I. Csonka, O. A. Vydrov, G. E. Scuseria, L. A. Constantin, X. Zhou, and K. Burke, "Restoring the density-gradient expansion for exchange in solids and surfaces," Phys. Rev. Lett. **100**, 136406 (2008).

[27] G. I. Csonka, J. P. Perdew, A. Ruzsinszky, P. H. T. Philipsen, S. Lebègue, J. Paier, O. A. Vydrov, and J. G. Ángyán, "Assessing the performance of recent density functionals for bulk solids," Phys. Rev. B **79**, 155107 (2009).

[28] Y. Kanai and J. C. Grossman, "Role of exchange in density-functional theory for weakly interacting systems: Quantum Monte Carlo analysis of electron density and interaction energy," Phys. Rev. A **80**, 032504 (2009).

[29] K. Yang, J. Zheng, Y. Zhao, and D. G. Truhlar, "Tests of the RPBE, revPBE, τ-HCTHhyb, ωB97X-D, and MOHLYP density functional approximations and 29 others against representative databases for diverse bond energies and barrier heights in catalysis," J. Chem. Phys. **132**, 164117 (2010).

[30] K. Berland, C. A. Arter, V. R. Cooper, K. Lee, B. I. Lundqvist, E. Schröder, T. Thonhauser, and P. Hyldgaard, "van der Waals density functionals built upon the electron-gas tradition: Facing the challenge of competing interactions," J. Chem. Phys. **140**, 18A539 (2014).

[31] I. Hamada and M. Otani, "Comparative van der Waals density-functional study of graphene on metal surfaces," Phys. Rev. B **82**, 153412 (2010).

[32] W. Liu, J. Carrasco, B. Santra, A. Michaelides, M. Scheffler, and A. Tkatchenko, "Benzene adsorbed on metals: Concerted effect of covalency and van der Waals bonding," Phys. Rev. B **86**, 245405 (2012).

[33] J. Klimeš, D. R. Bowler, and A. Michaelides, "Van der Waals density functionals applied to solids," Phys. Rev. B **83**, 195131 (2011).

[34] G.-X. Zhang, A. M. Reilly, A. Tkatchenko, and M. Scheffler, "Performance of various density-functional approximations for cohesive properties of 64 bulk solids," New J. Phys. **20**, 063020 (2018).

[35] D. Chakraborty, K. Berland, and T. Thonhauser, "Next-Generation Nonlocal van der Waals Density Functional," J. Chem. Theory Comput. **16**, 5893–5911 (2020).

[36] *Fundamentals of Time-Dependent Density Functional Theory*, Lecture Notes in Physics, edited by M. A. Marques, N. T. Maitra, F. M. Nogueira, E. Gross, and A. Rubio (Springer Berlin Heidelberg, Berlin, Heidelberg, 2012), Vol. 837.

[37] D. C. Langreth, M. Dion, H. Rydberg, E. Schröder, P. Hyldgaard, and B. I. Lundqvist, "Van der Waals density functional theory with applications," Int. J. Quantum Chem. **101**, 599–610 (2005).

[38] J. Klimeš, D. R. Bowler, and A. Michaelides, "Chemical accuracy for the van der Waals density functional," J. Phys.: Condens. Matter **22**, 022201 (2010).

[39] O. A. Vydrov and T. Van Voorhis, "Nonlocal van der Waals density functional made simple," Phys. Rev. Lett. **103**, 063004 (2009).

[40] O. A. Vydrov and T. Van Voorhis, "Nonlocal van der Waals density functional: The simpler the better," J. Chem. Phys. **133**, 244103 (2010).

[41] D. C. Langreth and S. Vosko, *Advances in Quantum Chemistry* (Elsevier, 1990), Vol. 21, pp. 175–199.

[42] J. P. Perdew and W. Yue, "Accurate and simple density functional for the electronic exchange energy: Generalized gradient approximation," Phys. Rev. B **33**, 8800–8802 (1986).

[43] P. Drude, "Zur Elektronentheorie der Metalle," Ann. Phys. **306**, 566–613 (1900).

[44] F. London, "The general theory of molecular forces," Trans. Faraday Soc. **33**, 8b (1937).

[45] A. Otero de la Roza and G. A. DiLabio, *Non-covalent Interactions in Quantum Chemistry and Physics: Theory and Applications* (Elsevier, Amsterdam, 2017).

[46] H. B. G. Casimir and D. Polder, "The Influence of retardation on the London-van der Waals forces," Phys. Rev. **73**, 360–372 (1948).

[47] V. G. Bezchastnov, M. Pernpointner, P. Schmelcher, and L. S. Cederbaum, "Nonadditivity and anisotropy of the polarizability of clusters: Relativistic finite-field calculations for the Xe dimer," Phys. Rev. A **81**, 062507 (2010).

[48] K. T. Tang and M. Karplus, "Padé-approximant calculation of the nonretarded van der Waals coefficients for two and three helium atoms," Phys. Rev. **171**, 70–74 (1968).

[49] K. T. Tang, "Dynamic polarizabilities and van der Waals coefficients," Phys. Rev. **177**, 108–114 (1969).

[50] T. Brinck, J. S. Murray, and P. Politzer, "Polarizability and volume," J. Chem. Phys. **98**, 4305–4306 (1993).

[51] V. G. Ruiz, W. Liu, and A. Tkatchenko, "Density-functional theory with screened van der Waals interactions applied to atomic and molecular adsorbates on close-packed and non-close-packed surfaces," Phys. Rev. B **93**, 035118 (2016).

[52] A. J. A. Price, K. R. Bryenton, and E. R. Johnson, "Requirements for an accurate dispersion-corrected density functional," J. Chem. Phys. **154**, 230902 (2021).

[53] E. R. McNellis, J. Meyer, and K. Reuter, "Azobenzene at coinage metal surfaces: Role of dispersive van der Waals interactions," Phys. Rev. B **80**, 205414 (2009).

[54] T. Bučko, S. Lebègue, J. G. Ángyán, and J. Hafner, "Extending the applicability of the Tkatchenko-Scheffler dispersion correction via iterative Hirshfeld partitioning," J. Chem. Phys. **141**, 034114 (2014).

[55] A. D. Becke and E. R. Johnson, "Exchange-hole dipole moment and the dispersion interaction," J. Chem. Phys. **122**, 154104 (2005).

[56] L. Salem, "The calculation of dispersion forces," Mol. Phys. **3**, 441–452 (1960).

[57] K. Pernal, R. Podeszwa, K. Patkowski, and K. Szalewicz, "Dispersionless density functional theory," Phys. Rev. Lett. **103**, 263201 (2009).

[58] R. J. Maurer, V. G. Ruiz, and A. Tkatchenko, "Many-body dispersion effects in the binding of adsorbates on metal surfaces," J. Chem. Phys. **143**, 102808 (2015).

[59] C. Gutle, A. Savin, J. B. Krieger, and J. Chen, "Correlation energy contributions from low-lying states to density functionals based on an electron gas with a gap," Int. J. Quantum Chem. **75**, 885–888 (1999).

[60] J. W. Furness and J. Sun, "Enhancing the efficiency of density functionals with an improved iso-orbital indicator," Phys. Rev. B **99**, 041119 (2019).

[61] S. Grimme, "Accurate description of van der Waals complexes by density functional theory including empirical corrections," J. Comput. Chem. **25**, 1463–1473 (2004).

[62] J.-D. Chai and M. Head-Gordon, "Long-range corrected hybrid density functionals with damped atom–atom dispersion corrections," Phys. Chem. Chem. Phys. **10**, 6615 (2008).

[63] D. G. A. Smith, L. A. Burns, K. Patkowski, and C. D. Sherrill, "Revised damping parameters for the D3 dispersion correction to density functional theory," J. Phys. Chem. Lett. **7**, 2197–2203 (2016).

[64] Q. Wu and W. Yang, "Empirical correction to density functional theory for van der Waals interactions," J. Chem. Phys. **116**, 515–524 (2002).

[65] E. R. Johnson and A. D. Becke, "A post-Hartree–Fock model of intermolecular interactions," J. Chem. Phys. **123**, 024101 (2005).

[66] S. Grimme, "Semiempirical GGA-type density functional constructed with a long-range dispersion correction," J. Comput. Chem. **27**, 1787–1799 (2006).

[67] P. Jurečka, J. Šponer, J. Černý, and P. Hobza, "Benchmark database of accurate (MP2 and CCSD(T) complete basis set limit) interaction energies of small model complexes, DNA base pairs, and amino acid pairs," Phys. Chem. Chem. Phys. **8**, 1985–1993 (2006).

[68] T. Takatani, E. G. Hohenstein, M. Malagoli, M. S. Marshall, and C. D. Sherrill, "Basis set consistent revision of the S22 test set of noncovalent interaction energies," J. Chem. Phys. **132**, 144104 (2010).

[69] F. Gao and L. Han, "Implementing the Nelder-Mead simplex algorithm with adaptive parameters," Comput. Optim. Appl. **51**, 259–277 (2012).

[70] P. Virtanen *et al.*, "SciPy 1.0: Fundamental algorithms for scientific computing in Python," Nat. Methods **17**, 261–272 (2020).

[71] M. A. Caro, "Parametrization of the Tkatchenko-Scheffler dispersion correction scheme for popular exchange-correlation density functionals: Effect on the description of liquid water," arXiv:1704.00761 [cond-mat] (2017).

[72] V. Blum, R. Gehrke, F. Hanke, P. Havu, V. Havu, X. Ren, K. Reuter, and M. Scheffler, "*Ab initio* molecular simulations with numeric atom-centered orbitals," Comput. Phys. Commun. **180**, 2175–2196 (2009).

[73] J. H. van Lenthe, S. Faas, and J. G. Snijders, Gradients in the ab initio scalar zeroth-order regular approximation žZORA/approach. 2000.

[74] S. Lehtola, C. Steigemann, M. J. Oliveira, and M. A. Marques, "Recent developments in libxc—A comprehensive library of functionals for density functional theory," SoftwareX **7**, 1–5 (2018).

[75] L. Gráfová, M. Pitoňák, J. Řezáč, and P. Hobza, "Comparative study of selected wave function and density functional methods for noncovalent interaction energy calculations using the extended S22 data set," J. Chem. Theory Comput. **6**, 2365–2376 (2010).

[76] B. Brauer, M. K. Kesharwani, S. Kozuch, and J. M. L. Martin, "The S66x8 benchmark for noncovalent interactions revisited: Explicitly correlated *ab initio* methods and density functional theory," Phys. Chem. Chem. Phys. **18**, 20905–20925 (2016).

[77] J. Řezáč, K. E. Riley, and P. Hobza, "S66: A well-balanced database of benchmark interaction energies relevant to biomolecular structures," J. Chem. Theory Comput. **7**, 2427–2438 (2011).

[78] R. A. DiStasio, V. V. Gobre, and A. Tkatchenko, "Many-body van der Waals interactions in molecules and condensed matter," J. Phys.: Condens. Matter **26**, 213202 (2014).

[79] R. Sedlak, T. Janowski, M. Pitoňák, J. Řezáč, P. Pulay, and P. Hobza, "Accuracy of quantum chemical methods for large noncovalent complexes," J. Chem. Theory Comput. **9**, 3364–3374 (2013).

[80] J. Řezáč, "Non-covalent interactions Atlas benchmark data sets 5: London dispersion in an extended chemical space," Phys. Chem. Chem. Phys. **24**, 14780–14793 (2022).

[81] M. Kim, W. J. Kim, T. Gould, E. K. Lee, S. Lebègue, and H. Kim, "uMBD: A materials-ready dispersion correction that uniformly treats metallic, ionic, and van der Waals bonding," J. Am. Chem. Soc. **142**, 2346–2354 (2020).

[82] H. B. Gray, *Chemical Bonds: An Introduction to Atomic and Molecular Structure* (University Science Books, 1994).

[83] R. Sure and S. Grimme, "Corrected small basis set Hartree-Fock method for large systems," J. Comput. Chem. **34**, 1672–1685 (2013).